



HAL
open science

Benchmark 3D: CeVe-DDFV, a discrete duality scheme with cell/vertex unknowns.

Yves Coudiere, Charles Pierre

► **To cite this version:**

Yves Coudiere, Charles Pierre. Benchmark 3D: CeVe-DDFV, a discrete duality scheme with cell/vertex unknowns.. Int. symposium on Finite Volumes for Complex Applications VI. Praha, 2011, May 2011, Praha, Czech Republic. pp.1-10. hal-00561980v2

HAL Id: hal-00561980

<https://hal.science/hal-00561980v2>

Submitted on 7 Mar 2011

HAL is a multi-disciplinary open access archive for the deposit and dissemination of scientific research documents, whether they are published or not. The documents may come from teaching and research institutions in France or abroad, or from public or private research centers.

L'archive ouverte pluridisciplinaire **HAL**, est destinée au dépôt et à la diffusion de documents scientifiques de niveau recherche, publiés ou non, émanant des établissements d'enseignement et de recherche français ou étrangers, des laboratoires publics ou privés.

Benchmark 3D: CeVe-DDFV, a Discrete Duality Scheme with Cell/Vertex Unknowns.

Yves Coudière and Charles Pierre

Abstract This paper presents numerical results for a 3D Cell and Vertex centered DDFV scheme. The method applies to very general 3D meshes including non conformal ones. Its construction and implementation are presented.

Key words: finite volume, discrete duality, gradient reconstruction
MSC2010: 65-06, 65N08, 65N12

1 Presentation of the scheme

1.1 General presentation of DDFV methods

“Discrete Duality” Finite Volumes (DDFV) schemes have been specifically designed for anisotropic and/or heterogeneous diffusion problems working on general meshes: distorted, non-conformal and locally refined. They first were introduced in 2D independently by Hermeline [9, 10] and Domelevo and Omnès [8], though the key ideas already appear in the work of Nicolaides [14].

As originally defined in [8], a 2D DDFV scheme consists in associating a second mesh (the dual mesh) to the original (primal) mesh by building dual cells around each (primal) mesh vertex. Cell and vertex centered *scalar data* are associated to this *double mesh* framework (one data per primal and dual cell), whereas a *vector data* consists in one vector per (primal) mesh edge. To a scalar data is associated a discrete gradient that is a vector data. A *gradient reconstruction* method is used

Yves Coudière
LMJL, Université de Nantes, France, e-mail: Yves.Coudiere@univ-nantes.fr

Charles Pierre
LMA, Université de Pau et des pays de l’Adour, France, e-mail: charles.pierre@univ-pau.fr

to define this discrete gradient: precisely using the diamond method [6]. A discrete divergence acts on vector data by averaging their normal component on the primal and dual cell boundaries, which procedure is classical for finite volume methods. The key feature is a duality property between the discrete gradient and the discrete divergence operators of Green formula type.

Extensions of *DDFV* schemes to 3D [15, 11, 12, 2, 3, 1, 3] are of two types.

CV-DDFV. The original 2D *double mesh* framework is conserved, dual cells are built around the primal mesh vertices and scalar data consist in a double set of unknowns associated with the (primal) mesh cells and vertices.

CeVeFE-DDFV. Recently Coudière and Hubert [4, 3] modified the 2D framework by considering a third mesh (triple mesh method), with unknowns associated with cells, faces, edges and vertices of the primal mesh.

The method considered here is of *CV-DDFV* type, *CV* holding for Cell and Vertex centered. Two versions have been developed so far.

- (A) A first 3D construction was introduced by Pierre in [15] for anisotropic and/or heterogeneous diffusion problems. The dual cells here do not form a mesh in the classical sense: they recover the domain twice.
- (B) A second version, independently introduced by Hermeline [12] and Andreianov & al. [2, 1] differs from the previous one by the dual cell definition that here form a partition of Ω .

For both versions, in presence of heterogeneity, auxiliary (locally eliminated) data are added relatively to faces, as presented in [5, 12]. In case of complex meshes, involving face shapes other than triangles or quadrangles, this local elimination procedure is made difficult enforcing to consider auxiliary data as real unknowns inside the algorithm, which drastically increases the problem size.

We first emphasize the similarities between (A) and (B). These two versions are based on the same definition of the discrete gradient. They also induce comparable discrete duality properties. Indeed, after a careful examination of these duality properties in [15] and in [2] it turns out that they do involve exactly the same stiffness and mass matrices. As a result, between these two versions, only the averaging of the source terms on the dual cells will differ.

In this paper, version (A) will be considered without auxiliary data on the mesh faces. The fifth test case, including heterogeneity and thus necessitating these auxiliary unknowns per face center, will not be treated here because of a lack of time.

1.2 *CV-DDFV version (A), discrete duality*

Let the domain $\Omega \subset \mathbb{R}^3$ be a connected open subset, its boundary is assumed to be polyhedral. Let \mathcal{M} be a (general) mesh of Ω , possibly non conformal, and whose (primal) cells (*resp.* faces) are general polyhedral (*resp.* polygonal). The set of cells, faces and vertices of \mathcal{M} are respectively denoted \mathcal{C} , \mathcal{F} and \mathcal{V} . To any vertex $v \in \mathcal{V}$

is associated a dual cell v^* and to any face $f \in \mathcal{F}$ is associated a diamond cell D_f . Diamond cells form a partition of Ω , whereas dual cells intersect and recover Ω exactly twice.

A vector data is a piecewise constant vector function on the diamond cells. A scalar data is provided by one scalar per cell and per vertex of \mathcal{M} . The space of vector data is denoted \mathbb{Q}_h and the space of scalar data \mathbb{F}_h . A discrete function is obtained by supplementing a scalar data with one scalar data per boundary face. The space of discrete functions is denoted \mathbb{U}_h . As developed in Sec. 1.3, $u_h \in \mathbb{U}_h$ will be interpreted as a function defined on the diamond cell boundaries:

$$\partial \mathcal{D} := \bigcup_{f \in \mathcal{F}} \partial D_f, \quad u_h : \partial \mathcal{D} \longrightarrow \mathbb{R}, \quad (1)$$

that moreover is continuous and piecewise affine on the diamond cell faces.

Two discrete operators will be defined, $\nabla_h : \mathbb{U}_h \longrightarrow \mathbb{Q}_h$ and $\text{div}_h : \mathbb{Q}_h \longrightarrow \mathbb{F}_h$. that satisfy the *discrete duality property* (see [15])

$$\int_{\Omega} \nabla_h u_h \cdot \mathbf{q}_h dx = -\langle \langle u_h, \text{div}_h \mathbf{q}_h \rangle \rangle + \int_{\partial \Omega} u_h \mathbf{q}_h \cdot \mathbf{n} ds \quad (2)$$

for any functions $u_h \in \mathbb{U}_h$ and $\mathbf{q}_h \in \mathbb{Q}_h$, with \mathbf{n} the unit normal on $\partial \Omega$ pointing outside Ω , and the pairing:

$$\langle \langle u_h, \text{div}_h \mathbf{q}_h \rangle \rangle = \frac{1}{3} \sum_{c \in \mathcal{C}} u_c \text{div}_c \mathbf{q}_h |c| + \frac{1}{3} \sum_{v \in \mathcal{V}} u_v \text{div}_v \mathbf{q}_h |v^*|. \quad (3)$$

Here, $|c|$ and $|v^*|$ are the volumes of the primal and dual cells c and v^* , u_c and $\text{div}_c \mathbf{q}_h$ are the values associated to the cell c of the two scalar data u_h and $\text{div}_h \mathbf{q}_h$, and similarly u_v and $\text{div}_v \mathbf{q}_h$ are the values associated to the vertex v of the two scalar data u_h and $\text{div}_h \mathbf{q}_h$.

In (2) the two integrals are well defined. The first integral is an L^2 product on Ω since both \mathbf{q}_h and $\nabla_h u_h$ are piecewise constant vector functions on the diamond cells. The second integral is an L^2 product on $\partial \Omega$: \mathbf{q}_h is piecewise constant on the boundary faces and its normal component $\mathbf{q}_h \cdot \mathbf{n}$ also, moreover $\partial \Omega \subset \partial \mathcal{D}$ defined in (1) and so u_h has a restriction to $\partial \Omega$ that is continuous.

1.3 Dual and diamond cells

A center x_c (resp. x_f) is associated to each cell $c \in \mathcal{C}$ (resp. $f \in \mathcal{F}$).

Diamond cells. Let $f \in \mathcal{F}$. In case $f \not\subset \partial \Omega$ then f is the interface between two cells $c_1, c_2 \in \mathcal{C}$: $f = \overline{c_1} \cap \overline{c_2}$. Denoting x_i the center of c_i , then D_f is the union of the two pyramids with apex x_i and with base f as depicted on Fig. 1. In case $f \subset \partial \Omega$, then $f = \partial \Omega \cap c$ for one cell $c \in \mathcal{C}$. In this case D_f is the pyramid with apex x_c and base f . Still in this cases, f can be considered as a degenerated (flat)

pyramid of apex its own center x_f and base f . Thus, in all cases, D_f is the union of two pyramids, and its boundary can be partitioned into triangles. The vertices of these triangles either are: cell centers, vertices or boundary face centers of \mathcal{M} . As a result providing a scalar value to each cell, vertex and boundary face of \mathcal{M} defines a unique continuous piecewise affine function $u_h : \partial\mathcal{D} \mapsto \mathbb{R}$, with $\partial\mathcal{D}$ defined in (1). This is precisely the lift from the discrete function in \mathbb{U}_h presented in Sec. 1.2 into continuous piecewise affine functions on $\partial\mathcal{D}$ in (1).

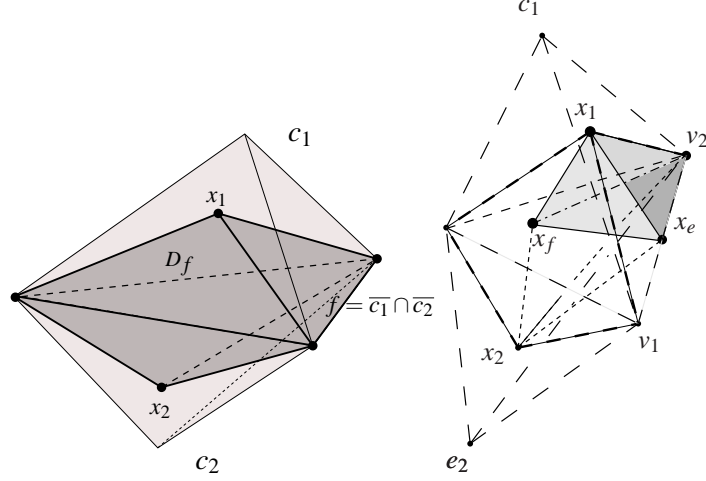


Fig. 1 Left: diamond cell for an internal triangular face f . Right: dual cell construction.

Dual cells. Let $v \in \mathcal{V}$ and consider a cell $c \in \mathcal{C}$ and a face $f \in \mathcal{F}$ so that v is a vertex of f and f is a face of c . This configuration is denoted by $v \prec f \prec c$. To a triple (v, f, c) so that $v \prec f \prec c$ is associated an element $T_{v,f,c}$. The dual cell v^* then is defined as $v^* = \bigcup_{f,c: v \prec f \prec c} T_{v,f,c}$. Let us eventually define the element $T_{v,f,c}$, as depicted on Fig. 1. Introduce w_1 and w_2 the two vertices of f such that $[v, w_1]$ and $[v, w_2]$ are two edges of f . Then $T_{v,f,c}$ is the union of the two tetrahedra $v x_c x_f w_i$ for $i=1, 2$.

As one can see, for a fixed face f and a fixed cell c such that $f \subset \partial c$, considering all elements $T_{v,f,c}$ for all the vertices v of f recovers exactly twice $D_f \cap c$. As a result the dual cells recover the whole domain exactly twice: $\sum_{v \in \mathcal{V}} |v^*| = 2|\Omega|$.

1.4 Discrete operators

The discrete divergence is classically defined by averaging the normal component of $\mathbf{q}_h \in \mathbb{Q}_h$ on the primal and dual cells, for all $c \in \mathcal{C}$ and all $v \in \mathcal{V}$:

$$\operatorname{div}_c \mathbf{q}_h = \frac{1}{|c|} \int_{\partial c} \mathbf{q}_h \cdot \mathbf{n} ds, \quad \operatorname{div}_v \mathbf{q}_h = \frac{1}{|v^*|} \int_{\partial v^*} \mathbf{q}_h \cdot \mathbf{n} ds, \quad (4)$$

for \mathbf{n} the unit normal on ∂c (resp. ∂v^*) pointing outside c (resp. v^*). This definition is well posed since the discontinuity set of $\mathbf{q}_h \in \mathbb{Q}_h$ has a zero 2-dimensional measure intersection with the primal and dual cell boundaries.

The discrete gradient is defined as follows. Let $u_h \in \mathbb{U}_h$, for all $f \in \mathcal{F}$:

$$\nabla_f u_h = \frac{1}{|D_f|} \int_{\partial D_f} u_h \mathbf{n} ds, \quad (5)$$

where $\nabla_f u_h$ is the (vector) value of $\nabla_h u_h$ on D_f and for \mathbf{n} the unit normal on ∂D_f pointing outside D_f .

In practice, definition (5) can always be reformulated in terms of data differences as in the 2D case where (see e.g. [7]):

$$\nabla_f u_h = (u_{c_1} - u_{c_2}) \mathbf{N}_f + (u_{v_1} - u_{v_2}) \mathbf{M}_f,$$

f is a mesh interface (edge), c_1 and c_2 the two cells on each side of f , v_1 and v_2 the two vertices of f and $\mathbf{N}_f, \mathbf{M}_f$ two vectors. We refer to [15, 5] for similar expansions in 3D.

1.5 The scheme

The linear diffusion problem $-\operatorname{div}(\mathbf{K} \nabla u) = f$ is considered together with a Dirichlet boundary condition $u|_{\partial \Omega} = g$. The tensor \mathbf{K} is discretized into \mathbf{K}_h by averaging \mathbf{K} on each diamond cells and the source term f is discretized as $f_h \in \mathbb{F}_h$ by averaging f over each primal and dual cells. The problem reads: find $u_h \in \mathbb{U}_h$ such that

$$\forall c \in \mathcal{C} : \operatorname{div}_c(\mathbf{K}_h \nabla_h u_h) = f_c, \quad \forall v \in \mathcal{V}, v \notin \partial \Omega : \operatorname{div}_v(\mathbf{K}_h \nabla_h u_h) = f_v \quad (6)$$

$$\forall v \in \mathcal{V}, v \in \partial \Omega : u_h(v) = g(v), \quad \forall f \in \mathcal{F}, f \subset \partial \Omega : u_h(x_f) = g(x_f), \quad (7)$$

To solve (6) (7), we split $\mathbb{U}_h = \mathbb{U}_{h,0} \oplus \mathbb{B}$ where $\mathbb{U}_{h,0}$ is the subset of discrete functions equal to zero on $\partial \Omega$. Then u_h decomposes as $u_h = u_0 + \tilde{u}$, where $\tilde{u} \in \mathbb{B}$ is uniquely determined by (7). Now $u_0 \in \mathbb{U}_{h,0}$ satisfies $-\operatorname{div}_h(\mathbf{K}_h \nabla_h u_0) = f_h + \operatorname{div}_h(\mathbf{K}_h \nabla_h \tilde{u}) := \tilde{f}_h$ for all primal cells and all interior vertices. This is a square linear system equivalent with: find $u_0 \in \mathbb{U}_{h,0}$ so that for all $v \in \mathbb{U}_{h,0}$ we have:

$$-\langle \operatorname{div}_h(\mathbf{K}_h \nabla_h u_0), v \rangle = \langle \tilde{f}_h, v \rangle$$

With the help of the discrete duality property (2) it is also equivalent with finding $u_0 \in \mathbb{U}_{h,0}$ so that for all $v \in \mathbb{U}_{h,0}$:

$$\int_{\Omega} \mathbf{K}_h \nabla_h u_0 \cdot \nabla_h v dx = \langle \tilde{f}_h, v \rangle.$$

In practice, introducing the stiffness matrix S associated to the discrete tensor \mathbf{K}_h , this problem is rewritten as the square positive symmetric linear system

$$SU_0 = \tilde{F}, \quad (8)$$

with U_0 (resp. \tilde{F}) the vector formed by the values of u_0 (resp. \tilde{f}_h) at the cell centers and interior vertices. The stiffness matrix S has the coefficients $S_{ij} = \int_{\Omega} \mathbf{K}_h \nabla_h w_i \cdot \nabla_h w_j dx$, with $w_i \in \mathbb{U}_{h,0}$ the base function having value 1 at one cell center or interior vertex and 0 everywhere else. This matrix is clearly symmetric and positive.

2 Numerical results

The cell centers as well as the face centers are set to their iso-barycenter.

Let us first define the data (source term f and anisotropy tensor \mathbf{K}) discretization. Primal, dual and diamond cells are partitioned using a single set of tetrahedra of type $E = x_c x_f v_1 v_2$, with $c \in \mathcal{C}$, f a face of c and v_1, v_2 two vertices of f forming one of its edges. To form the scalar data f_h , f is averaged on the tetrahedra E partitioning each primal and dual cells whereas the discrete tensor \mathbf{K}_h is obtained by averaging \mathbf{K} on the tetrahedra E partitioning the diamond cells. Averaging is made by the mean of Gaussian quadrature on each tetrahedra E using a 15 points quadrature formula of order 5, see e.g. [13]. Assembling the discrete source term f_h and tensor \mathbf{K}_h requires one loop on the mesh faces.

The stiffness matrix S in (8) also is assembled using a loop on the mesh faces. Precisely two base functions w_i and w_j have a non zero interaction (i.e. $S_{ij} = \int_{\Omega} \mathbf{K}_h \nabla_h w_i \cdot \nabla_h w_j dx \neq 0$) in case they are associated to two vertices of a same diamond D_f .

Let us now define the L^2 , H^1 and energy errors reported in the following tables as erl2, ergrad and ener respectively. Let u_h denote the discrete solution of one of the test case, and u the solution of the associated continuous problem. The discrete function u_h is lifted to a function $\bar{u}_h \in L^2(\Omega)$ as follows. Consider a face f , u_h provides a value at each vertex of D_f and also at the face center x_f in case of a boundary face. In case of an interior face, a supplementary value u_f is computed at x_f as $u_f = (\sum_{i=1}^n u_{v_i})/n$ where the v_i are the n vertices of f , which definition is consistent since x_f is the iso-barycenter of f . With these additional values, scalars are available for every vertices of the tetrahedra E that partition Ω : this defines a unique function \bar{u}_h by P^1 interpolation, which then is continuous piecewise affine on Ω . We define:

$$\text{erl2}^2 = \frac{\int_{\Omega} |\bar{u}_h - u|^2 dx}{\int_{\Omega} |u|^2 dx}.$$

The discrete vector data $\nabla_h u_h$ is a piecewise constant vector function on the diamond cells. Therefore $\nabla_h u_h$ is an L^2 functions on Ω and the H^1 and energy errors reported in the following tables are defined as:

$$\text{ergrad}^2 = \frac{\int_{\Omega} |\nabla_h u_h - \nabla u|^2 dx}{\int_{\Omega} |\nabla u|^2 dx}, \quad \text{ener}^2 = \frac{\int_{\Omega} K(\nabla_h u_h - \nabla u) \cdot (\nabla_h u_h - \nabla u)}{\int_{\Omega} K \nabla u \cdot \nabla u dx}.$$

- **Test 1 Mild anisotropy**, $u(x, y, z) = 1 + \sin(\pi x) \sin(\pi(y + \frac{1}{2})) \sin(\pi(z + \frac{1}{3}))$
min = 0, max = 2, **Tetrahedral meshes**

i	nu	nmat	umin	uemin	umax	uemax	normg
1	2187	21287	1.34E-02	1.53E-02	1.99E+00	1.99E+00	1.80E+00
2	4301	44813	3.24E-03	6.84E-03	1.99E+00	1.99E+00	1.80E+00
3	8584	94088	8.78E-03	7.44E-03	2.00E+00	1.99E+00	1.80E+00
4	17102	195074	4.74E-03	5.52E-03	2.00E+00	2.00E+00	1.80E+00
5	34343	405077	5.90E-04	1.49E-03	2.00E+00	2.00E+00	1.80E+00
6	69160	838856	1.30E-03	6.19E-04	2.00E+00	2.00E+00	1.80E+00

i	nu	erl2	ratio12	ergrad	ratioegrad	ener	ratioener
1	2187	1.39E-02	-	1.85E-01	-	1.80E-01	-
2	4301	8.80E-03	2.04E+00	1.48E-01	1.01E+00	1.44E-01	9.89E-01
3	8584	5.64E-03	1.93E+00	1.18E-01	9.73E-01	1.15E-01	9.97E-01
4	17102	3.61E-03	1.94E+00	9.36E-02	1.01E+00	9.10E-02	1.01E+00
5	34343	2.26E-03	2.01E+00	7.43E-02	9.92E-01	7.24E-02	9.81E-01
6	69160	1.42E-03	2.00E+00	5.87E-02	1.01E+00	5.70E-02	1.02E+00

- **Test 1 Mild anisotropy**, $u(x, y, z) = 1 + \sin(\pi x) \sin(\pi(y + \frac{1}{2})) \sin(\pi(z + \frac{1}{3}))$
min = 0, max = 2, **Voronoi meshes**

i	nu	nmat	umin	uemin	umax	uemax	normg
1	87	1433	1.23E-01	1.79E-01	1.91E+00	1.85E+00	1.80E+00
2	235	4393	6.66E-02	2.93E-03	1.87E+00	2.00E+00	1.80E+00
3	527	10777	1.32E-02	9.56E-03	1.93E+00	1.97E+00	1.80E+00
4	1013	21793	-1.76E-03	4.97E-03	1.93E+00	2.00E+00	1.80E+00
5	1776	40998	5.42E-04	4.30E-03	1.98E+00	1.97E+00	1.80E+00

i	nu	erl2	ratio12	ergrad	ratioegrad	ener	ratioener
1	87	6.19E-02	-	4.43E-01	-	4.29E-01	-
2	235	3.36E-02	1.85E+00	3.37E-01	8.28E-01	3.29E-01	7.96E-01
3	527	2.10E-02	1.74E+00	2.55E-01	1.03E+00	2.49E-01	1.04E+00
4	1013	1.35E-02	2.03E+00	2.05E-01	1.01E+00	2.01E-01	9.85E-01
5	1776	9.99E-03	1.62E+00	1.75E-01	8.38E-01	1.71E-01	8.47E-01

- **Test 1 Mild anisotropy**, $u(x, y, z) = 1 + \sin(\pi x) \sin\left(\pi\left(y + \frac{1}{2}\right)\right) \sin\left(\pi\left(z + \frac{1}{3}\right)\right)$
min = 0, max = 2, **Kershaw meshes**

i	nu	nmat	umin	uemin	umax	uemax	normg
1	855	13819	7.16E-02	2.88E-02	1.94E+00	1.96E+00	1.80E+00
2	7471	138691	1.26E-02	6.45E-03	1.99E+00	1.99E+00	1.80E+00
3	62559	1237459	1.30E-03	1.75E-03	2.00E+00	2.00E+00	1.80E+00
4	512191	10443763	4.61E-04	5.45E-04	2.00E+00	2.00E+00	1.80E+00

i	nu	erl2	ratio12	ergrad	ratiograd	ener	ratioener
1	855	5.64E-02	-	4.57E-01	-	4.51E-01	-
2	7471	1.71E-02	1.65E+00	1.91E-01	1.20E+00	1.89E-01	1.21E+00
3	62559	3.45E-03	2.26E+00	7.74E-02	1.28E+00	7.67E-02	1.27E+00
4	512191	7.62E-04	2.15E+00	3.47E-02	1.14E+00	3.41E-02	1.16E+00

- **Test 1 Mild anisotropy**, $u(x, y, z) = 1 + \sin(\pi x) \sin\left(\pi\left(y + \frac{1}{2}\right)\right) \sin\left(\pi\left(z + \frac{1}{3}\right)\right)$
min = 0, max = 2, **Checkerboard meshes**

i	nu	nmat	umin	uemin	umax	uemax	normg
1	59	703	1.46E-01	3.41E-02	1.86E+00	1.97E+00	1.80E+00
2	599	9835	3.87E-02	8.56E-03	1.96E+00	1.99E+00	1.80E+00
3	5423	101539	9.24E-03	2.14E-03	1.99E+00	2.00E+00	1.80E+00
4	46175	917395	2.15E-03	5.35E-04	2.00E+00	2.00E+00	1.80E+00
5	381119	7788403	5.01E-04	1.34E-04	2.00E+00	2.00E+00	1.80E+00

i	nu	erl2	ratio12	ergrad	ratiograd	ener	ratioener
1	59	4.79E-02	-	4.01E-01	-	3.94E-01	-
2	599	1.08E-02	1.93E+00	1.95E-01	9.34E-01	1.92E-01	9.31E-01
3	5423	2.55E-03	1.96E+00	9.58E-02	9.66E-01	9.37E-02	9.73E-01
4	46175	6.27E-04	1.96E+00	4.75E-02	9.83E-01	4.63E-02	9.89E-01
5	381119	1.56E-04	1.98E+00	2.36E-02	9.92E-01	2.30E-02	9.95E-01

- **Test 2 Heterogeneous anisotropy**,
 $u(x, y, z) = x^3 y^2 z + x \sin(2\pi x z) \sin(2\pi x y) \sin(2\pi z)$, min = -0.862, max = 1.0487,
Prism meshes

i	nu	nmat	umin	uemin	umax	uemax	normg
1	3010	64158	-8.54E-01	-8.41E-01	1.00E+00	1.00E+00	1.71E+00
2	24020	555528	-8.56E-01	-8.59E-01	1.02E+00	1.05E+00	1.71E+00
3	81030	1924098	-8.61E-01	-8.59E-01	1.04E+00	1.04E+00	1.71E+00
4	192040	4619868	-8.59E-01	-8.61E-01	1.04E+00	1.05E+00	1.71E+00

i	nu	erl2	ratio2	ergrad	ratiograd	ener	ratioener
1	3010	5.06E-02	-	2.45E-01	-	2.48E-01	-
2	24020	1.85E-02	1.45E+00	1.26E-01	9.63E-01	1.27E-01	9.66E-01
3	81030	1.46E-02	5.90E-01	8.51E-02	9.63E-01	8.59E-02	9.66E-01
4	192040	1.37E-02	2.08E-01	6.49E-02	9.44E-01	6.53E-02	9.50E-01

- **Test 3 Flow on random meshes, $u(x, y, z) = \sin(2\pi x) \sin(2\pi y) \sin(2\pi z)$, $\min = -1$, $\max = 1$, Random meshes**

i	nu	nmat	umin	uemin	umax	uemax	normg
1	91	1063	-1.58E+00	-9.78E-01	1.54E+00	9.31E-01	3.65E+00
2	855	13819	-1.08E+00	-9.94E-01	1.12E+00	9.82E-01	3.57E+00
3	7471	138691	-1.04E+00	-9.95E-01	1.01E+00	9.91E-01	3.60E+00
4	62559	1237459	-1.01E+00	-9.98E-01	1.01E+00	9.98E-01	3.60E+00

i	nu	erl2	ratio2	ergrad	ratiograd	ener	ratioener
1	91	3.06E-01	-	5.89E-01	-	5.70E-01	-
2	855	8.29E-02	1.75E+00	3.14E-01	8.56E-01	2.87E-01	9.21E-01
3	7471	2.28E-02	1.79E+00	1.65E-01	8.90E-01	1.46E-01	9.28E-01
4	62559	6.98E-03	1.67E+00	8.96E-02	8.58E-01	7.34E-02	9.68E-01

- **Test 4 Flow around a well, Well meshes, $\min = 0$, $\max = 5.415$**

i	nu	nmat	umin	uemin	umax	uemax	normg
1	1482	23942	4.85E-01	-6.02E-06	5.32E+00	5.42E+00	1.62E+03
2	3960	70872	2.71E-01	-5.68E-06	5.33E+00	5.42E+00	1.62E+03
3	9229	173951	1.66E-01	-5.76E-06	5.33E+00	5.42E+00	1.62E+03
4	21156	412240	1.25E-01	-7.39E-06	5.33E+00	5.42E+00	1.62E+03
5	44420	882520	9.37E-02	-6.93E-06	5.34E+00	5.42E+00	1.62E+03
6	82335	1654893	7.48E-02	-6.94E-06	5.35E+00	5.42E+00	1.62E+03
7	145079	2937937	5.80E-02	-8.05E-06	5.36E+00	5.42E+00	1.62E+03

i	nu	erl2	ratio2	ergrad	ratiograd	ener	ratioener
1	1482	2.92E-03	-	1.79E-01	-	1.78E-01	-
2	3960	1.38E-03	2.29E+00	1.22E-01	1.18E+00	1.21E-01	1.16E+00
3	9229	7.45E-04	2.19E+00	8.57E-02	1.25E+00	8.56E-02	1.24E+00
4	21156	5.53E-04	1.08E+00	6.56E-02	9.71E-01	6.55E-02	9.72E-01
5	44420	3.77E-04	1.55E+00	5.14E-02	9.85E-01	5.13E-02	9.83E-01
6	82335	2.44E-04	2.11E+00	4.18E-02	1.01E+00	4.17E-02	1.01E+00
7	145079	1.83E-04	1.53E+00	3.51E-02	9.27E-01	3.50E-02	9.26E-01

3 Comments

The linear system (8) to be solved is symmetric and positive: a Conjugate Gradient algorithm has been applied, together with a basic Jacobi preconditioner. The sparsity pattern of the stiffness matrix is not compact, especially for matrix lines corresponding to vertex nodes. The stiffness matrix lines corresponding to cell nodes have $1 + n_f + n_s$ nonzero terms with n_f and n_v the number of faces and vertices of the considered cell; for a tetrahedra $1 + n_f + n_v = 9$. The maximum principle is not fulfilled by *DDFV* schemes. In practice it has been violated only once for test one on Voronoï meshes and more significantly on test 3. Meanwhile no oscillation phenomena are observed. Expected order 2 convergence on *erl2* is observed for all tests excepted test 2. Order 1 convergence is observed for *ergrad* and *ener* on all tests.

References

1. Andreianov, B., Bendahmane, M., Karlsen, K.H.: A gradient reconstruction formula for finite volume schemes and discrete duality. Proceedings of FVCA5 (2008)
2. Andreianov, B., Bendahmane, M., Karlsen, K.H.: Discrete duality finite volume schemes for doubly nonlinear degenerate hyperbolic-parabolic equations. *J. Hyperbolic Differ. Equ.* **7**(1), 1–67 (2010)
3. Coudière, Y., Hubert, F.: A 3d discrete duality finite volume method for nonlinear elliptic equation. HAL Preprint URL <http://hal.archives-ouvertes.fr/docs/00/45/68/37/PDF/ddfv3d.pdf>
4. Coudière, Y., Hubert, F.: A 3d duality finite volume method for nonlinear elliptic equations. Proceedings of Algoritmy 2009 pp. 51–60 (2009)
5. Coudiere, Y., Pierre, C., Rousseau, O., Turpault, R.: 2D/3D DDFV scheme for anisotropic-heterogeneous elliptic equations, application to electrograms simulation from medical data. *Int. J. Finite Volumes* (2009)
6. Coudière, Y., Vila, J.P., Villedieu, P.: Convergence rate of a finite volume scheme for a two dimensional convection-diffusion problem. *M2AN* **33**(3), 493–516 (1999)
7. Delcourte, S., Domelevo, K., Omnès, P.: Discrete-duality finite volume method for second order elliptic problems. Proceedings of FVCA4 pp. 447–458 (2005)
8. Domelevo, K., Omnes, P.: A finite volume method for the Laplace equation on almost arbitrary two-dimensional grids. *M2AN Math. Model. Numer. Anal.* **39**(6), 1203–1249 (2005)
9. Hermeline, F.: Une méthode de volumes finis pour les équations elliptiques du second ordre. *C. R. Acad. Sci.* **326**(12), 1433–1436 (1998)
10. Hermeline, F.: A finite volume method for the approximation of diffusion operators on distorted meshes. *J. Comput. Phys.* **160**(2), 481–499 (2000)
11. Hermeline, F.: Approximation of 2-D and 3-D diffusion operators with variable full tensor coefficients on arbitrary meshes. *Comput. Methods Appl. Mech. Engrg.* **196**(21-24), 2497–2526 (2007)
12. Hermeline, F.: A finite volume method for approximating 3D diffusion operators on general meshes. *Comput. Meth. Appl. Mech. Engrg.* (2009)
13. Jinyun, Y.: Symmetric gaussian quadrature formulae for tetrahedral regions. *Computer Methods in Applied Mechanics and Engineering* (1981)
14. Nicolaidis, R.: Direct discretization of planar div-curl problems. *SIAM J. Numer. Anal.* **29**(1), 32–56 (1992)
15. Pierre, C.: Modelling and simulating the electrical activity of the heart embedded in the torso, numerical analysis and finite volumes methods. . PhD Thesis, Université de Nantes (2005)

The paper is in final form and no similar paper has been or is being submitted elsewhere.